GRG manuscript No.
(will be inserted by the editor)

The second order spin-2 system in flat space near space-like and null-infinity

Georgios Doulis · **Jörg Frauendiener**

January 21, 2013

Abstract In previous work, the numerical solution of the linearized gravitational field equations near space-like and null-infinity was discussed in the form of the spin-2 zero-rest-mass equation for the perturbations of the conformal Weyl curvature. The motivation was to study the behavior of the field and properties of the numerical evolution of the system near infinity using Friedrich's conformal representation of space-like infinity as a cylinder. It has been pointed out by H.O. Kreiss and others that the numerical evolution of a system using second order wave equations has several advantages compared to a system of first order equations. Therefore, in the present paper we derive a system of second order wave equations and prove that the solution spaces of the two systems are the same if appropriate initial and boundary data are given. We study the properties of this system of coupled wave equations in the same geometric setting and discuss the differences between the two approaches.

1 Introduction

In a recent paper [1] we studied the behaviour of gravitational perturbations on Minkowski space near space-like infinity. For this purpose we used the spin-2 zero-rest-mass equation which governs the perturbations of the Weyl curvature. The system was studied using a conformal gauge given by Friedrich [6] which represents space-like infinity as a cylinder connecting past and future null-infinity. This gauge exhibits explicitly the main issues of the propagation of gravitational waves in asymptotically flat space-times, namely the question of how $\mathscr{I}^+$ is related to $\mathscr{I}^-$, or, in other words, how the late ingoing gravitational radiation affects the early outgoing radiation.

Georgios Doulis
Department of Mathematics and Statistics, University of Otago, Dunedin 9010, New Zealand
E-mail: gdoulis@maths.otago.ac.nz

Jörg Frauendiener
Department of Mathematics and Statistics, University of Otago, Dunedin 9010, New Zealand
E-mail: joergf@maths.otago.ac.nz

In [1] it was shown how the field propagates near the cylinder. It turns out that the cylinder is a total characteristic in the sense that the equations turn into intrinsic equations on it, there appear no outward derivatives. Hence, the field on the cylinder is entirely determined by initial data on a space-like initial hyper-surface and there are no free data to be prescribed on the cylinder.

The crucial property, however, is the fact that the intrinsic equations degenerate on the intersections $I^{\pm}$ between the cylinder and null-infinity $\mathscr{I}^{\pm}$. Here, the field may develop singularities which can propagate onto null-infinity destroying its smoothness. Friedrich has conjectured that certain conditions on the initial data have to be satisfied in order for the field to be smooth on $\mathscr{I}$.

These analytical properties have been explored numerically in [1] based on the first order system for the spin-2 field. The behavior of the resulting numerical solutions near the cylinder I was studied. The performance of the code near the ill-behaved location I^+ at the junction of the cylinder and null-infinity was tested using different initial data. The analytical results were reproduced quite successfully. In particular, the analytically predicted singular behaviour could be reproduced numerically. The results in [1] strongly indicate that appropriate classes of initial data can be successfully evolved without loss of convergence up and including the region I^+, but not beyond. As expected, since the equations are no longer hyperbolic beyond I^+ the code develops numerical instabilities and crashes.

With the present article we want to follow up on this work using an equivalent system of second order wave equations. Our main motivation for this is the claim by several numerical analysts (see e.g., Kreiss and Ortiz [9]) that the numerical solutions of second order wave equations have better properties that those for the corresponding first order systems.

The structure of the paper is as follows. In sec. 2 we briefly describe Friedrich's representation of space-like infinity of Minkowski space as a cylinder. In sec. 3 we derive the system of wave equations and show under what conditions it is equivalent to the first order system used in [1]. In sec. 4 our numerical implementation and results are presented. Finally, we conclude with a discussion in sec. 5. The conventions used in this work are those of [17].

2 The finite representation of Minkowski space-time near space-like infinity

In this section, we will briefly summarize the finite representation of Minkowski space-time close to space-like infinity originally proposed by Friedrich in [6]; more detailed discussions of this topic can be found in [1, 6, 20].

The physical metric of Minkowski space-time in Cartesian coordinates (y^μ) reads

$$\tilde{g} = \eta_{\mu\nu}\, \mathbf{d}y^\mu\, \mathbf{d}y^\nu,$$

where $\eta_{\mu\nu} = \mathrm{diag}(1,-1,-1,-1)$. In this representation the region that we are mainly interested in, namely the neighborhood of space-like infinity i^0, lies far away from the origin. In order to get a more detailed description of the points lying at infinity, we consider the coordinate inversion [16]: $y^\mu = -\frac{\mathrm{x}^\mu}{\mathrm{x}_\lambda\, \mathrm{x}^\lambda}$ which brings our original metric

into the form

$$\tilde{g} = \frac{1}{(\mathrm{x}_\lambda\, \mathrm{x}^\lambda)^2}\, \eta_{\mu\nu}\, \mathbf{d}\mathrm{x}^\mu\, \mathbf{d}\mathrm{x}^\nu.$$

Notice that with the aforementioned inversion points close to infinity in our original coordinates y^μ are now lying in the vicinity of the origin of the new 'inverted' coordinates x^μ. But this comes at a price: the above metric is singular at the null-cone of the origin $\mathrm{x}^\mu = 0$. Introducing the conformal factor

$$\Omega = -\mathrm{x}_\lambda\, \mathrm{x}^\lambda,$$

one can define the conformally equivalent metric

$$g' = \Omega^2 \tilde{g} = \eta_{\mu\nu}\, \mathbf{d}\mathrm{x}^\mu\, \mathbf{d}\mathrm{x}^\nu,$$

which extends smoothly to the null-cone $\mathrm{x}^\mu \mathrm{x}_\mu = 0$. This implies that space-like infinity is a regular point in Minkowski space-time. It is well-known that in space-times with non-vanishing ADM-mass this is no longer the case and space-like infinity can no longer be represented as a point. Instead, as discussed in detail in [6] it is more appropriate to represent the region near the origin as a cylinder. This is achieved here by a further rescaling of the metric

$$g = \kappa^{-2} g'$$

with a function $\kappa(r) = r\mu(r)$ where $r = \sqrt{(\mathrm{x}^1)^2 + (\mathrm{x}^2)^2 + (\mathrm{x}^3)^2}$ is the radial spatial distance from the origin and $\mu(r)$ is a positive radial function with $\mu(0) = 1$. The choice of the function μ represents the remaining conformal gauge freedom. After the introduction of a new time-coordinate t by defining $x^0 = \kappa(r)t$ the metric g expressed in polar coordinates takes the following spherically symmetric form

$$g = \kappa^{-2} \left(\kappa^2 \mathrm{d}t^2 + 2t\,\kappa\,\kappa' \mathrm{d}t\,\mathrm{d}r - (1 - t^2\,\kappa'^2)\mathrm{d}r^2 - r^2(\mathrm{d}\theta^2 + \sin^2\theta\,\mathrm{d}\phi^2)\right), \qquad (2.1)$$

where (θ, ϕ) are the usual angular coordinates and $'$ denotes differentiation with respect to the radial coordinate r. Notice that the final rescaled metric (2.1) and the original Minkowski $\tilde{g}$ are related by the conformal factor

$$\Theta = \kappa^{-1}\, \Omega = \frac{r}{\mu(r)}\, (1 - t^2\, \mu(r)^2),$$

which is positive on $M = \{r > 0, |t| < 1/\mu(r)\}$, corresponding to the Minkowski space-time. The conformal factor vanishes on the two regular 3-dimensional hyper-surfaces

$$\mathscr{I}^\pm = \{r > 0, t = \pm \frac{1}{\mu(r)}\} \qquad \text{and} \qquad I = \{r = 0,\, |t| < 1\}.$$

The hyper-surfaces $\mathscr{I}^\pm$ are null, corresponding to null-infinity, while I is a regular hyper-surface with the topology of a cylinder. Interestingly, in the limit $r \to 0$ future and past null-infinity do not meet at the same point as in the conventional picture. Instead, they meet the cylinder I in the 2-spheres $I^\pm = \{r = 0, t = \pm 1\}$. This observation leads naturally to the finite representation of space-like infinity, where i^0 has

been blown up to the cylinder $I = \{r = 0, -1 < t < 1\}$. The function μ dictates the shape of these structures. Here, the two simplest choices will be considered: $\mu(r) = 1$ and $\mu(r) = \frac{1}{1+r}$. In the former 'horizontal' representation, null-infinity is given by the set $\mathscr{I}^{\pm} = \{r > 0, t = \pm 1\}$, while in the latter 'diagonal' representation by the set $\mathscr{I}^{\pm} = \{r > 0, t = \pm(1+r)\}$, see Fig. 1. It is helpful to introduce the double null

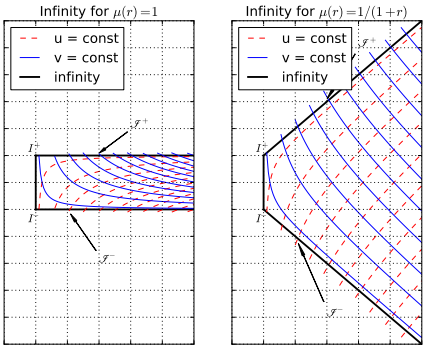

Fig. 1 The neighborhood of the cylinder I for the horizontal and the diagonal conformal representations.

coordinates

$$u = \kappa(r)t - r, \qquad v = \kappa(r)t + r, \tag{2.2}$$

which puts the metric into the form

$$g = \frac{1}{\kappa^2}\mathrm{d}u\mathrm{d}v - \frac{1}{\mu^2}\mathrm{d}\omega^2.$$

Now, $\mathscr{I}^{\pm}$ is characterized by the vanishing of exactly one of the null coordinates, the other one being non-zero. Both coordinates vanish on the cylinder I. In Fig. 1 we also display the lines of constant u and v. Since these are coordinates adapted to the conformal structure of M we can see clearly, that the cylinder is 'invisible' from the point of view of the conformal structure. Notice, that the differentiable structures defined by the (u,v) and the (t,r) coordinates are completely different near the boundary $r = 0$.

3 The spin-2 wave system

Our objectives in the present section are to derive a second order system for the spin-2 equation described in [1] and to establish a correspondence between the two formulations.

3.1 The spin-2 wave equation

Our starting point will be the spin-2 zero-rest-mass equation [16] on an arbitrary space-time

$$\nabla^{E}{}_{A'}\phi_{EBCD} = 0. \tag{3.1}$$

Acting on (3.1) with another spinorial covariant derivative $\nabla_{AA'}$ yields

$$0 = \nabla_{AA'}\nabla^{EA'}\phi_{EBCD} = \frac{1}{2}\Box\phi_{ABCD} + 3\Psi_{A(B}{}^{EF}\phi_{CD)EF} + 6\Lambda\phi_{ABCD}. \tag{3.2}$$

In the present case, the Weyl spinor vanishes, since the metric (2.1) is conformally flat. The Ricci tensor of this metric turns out to be trace-free, so that also $\Lambda = 0$. Thus, we obtain the wave equation

$$\Box\phi_{ABCD} = 0. \tag{3.3}$$

3.2 Relating the first with the second order system

Now, we will relate the first (3.1) with the second (3.3) order system. Establishing this correspondence is necessary because we need to know under what conditions we obtain the same solutions. We will then also be able to compare the numerical behavior of the two systems and study their similarities and differences. In the following, we will prove that in a conformally flat space-time with vanishing Ricci scalar a solution ϕ_{ABCD} of the spin-2 wave equation (3.3), which satisfies initially the spin-2 zero-rest-mass equation (3.1), is also a solution of the latter.

First, we define the spinor

$$\Sigma_{A'BCD} \equiv \nabla^{F}{}_{A'}\phi_{FBCD}. \tag{3.4}$$

Then the equation $\Sigma_{A'BCD} = 0$ is nothing else than the spin-2 equation (3.1). Rewriting (3.2), we obtain an equation for the derivative of $\Sigma_{A'BCD}$

$$\nabla_{AA'}\Sigma^{A'}{}_{BCD} = \frac{1}{2}\Box\phi_{ABCD} + 3\Psi_{A(B}{}^{EF}\phi_{CD)EF} + 6\Lambda\phi_{ABCD}. \tag{3.5}$$

Now, assume that ϕ_{ABCD} satisfies (3.1), then $\Sigma_{A'BCD} = 0$ and

$$\frac{1}{2}\Box\phi_{ABCD} + 3\Psi_{A(B}{}^{EF}\phi_{CD)EF} + 6\Lambda\phi_{ABCD} = 0.$$

Contracting over indices A and B yields

$$\Psi_{(C}{}^{AEF}\phi_{D)AEF} = 0,$$

a purely algebraic condition between the conformal curvature and the spinor field. This is a Buchdahl condition [17] which implies the well-known fact that the zero-rest mass equation (with spin 2 in this case) is inconsistent on space-times with non-vanishing Weyl tensor. So we take $\Psi_{ABCD} = 0$ from now on and we also assume that $\Lambda = 0$. Then the spinor field satisfies the second order wave equation

$$\Box\phi_{ABCD} = 0. \tag{3.6}$$

Conversely, let ϕ_{ABCD} be a solution of (3.3). Then (3.5) shows that the spinor field $\Sigma_{A'BCD} = 0$ satisfies the equation

$$\nabla_{AA'}\Sigma^{A'}{}_{BCD} = 0. \tag{3.7}$$

In order to study the properties of this system of PDE we look at its symbol. This is, for every real co-vector $p_{AA'}$, defined as a map $P : \mathscr{S}^{A'} \otimes \mathscr{S}_{(BCD)} \to \mathscr{S}_A \otimes \mathscr{S}_{(BCD)}$ between the appropriate spin spaces defined by

$$\alpha^{A'}\beta_{BCD} \mapsto p_{AA'}\alpha^{A'}\beta_{BCD}.$$

Therefore, it is enough to discuss only the map

$$\alpha^{A'} \mapsto p_{AA'}\alpha^{A'}. \tag{3.8}$$

Choosing a spin basis $(o^{A'}, \iota^{A'})$ in $\mathscr{S}^{A'}$ and the corresponding basis $(-\iota_A, o_A)$ in $\mathscr{S}_A$ and expanding $p_{AA'}$ as

$$p_{AA'} = p_0(o_A o_{A'} + \iota_A \iota_{A'}) - p_1(o_A \iota_{A'} + o_A \iota_{A'}) - \mathfrak{i} p_2(o_A \iota_{A'} - o_A \iota_{A'}) - p_3(o_A o_{A'} - \iota_A \iota_{A'})$$

with real $p_0, \dots, p_3$ we find the matrix representation of the map (3.8)

$$\begin{pmatrix} p_0 + p_3 & p_1 - \mathfrak{i} p_2 \\ p_1 + \mathfrak{i} p_2 & p_0 - p_3 \end{pmatrix}$$

which is clearly hermitian for every choice of co-vector $p_{AA'}$ and it is positive definite for the co-vector with $p_1 = p_2 = p_3 = 0$, $p_0 = 1$. The matrix representation of the map P then simply consists of four copies of this matrix along the diagonal. Thus, the system (3.7) is symmetric hyperbolic and its Cauchy problem is well-posed.

Thus, if $\Sigma_{A'BCD} = 0$ on an initial hyper-surface and, for initial boundary value problems, if boundary data are given such that the ingoing $\Sigma_{A'BCD}$ waves vanish, then the field $\Sigma_{A'BCD}$ vanishes everywhere, i.e., the field ϕ_{ABCD} satisfies (3.1). This conclusion holds on the region where the systems are hyperbolic. In our application below we will consider situations where hyperbolicity is lost on a region with codimension 2, namely the spheres $I^{\pm}$. We find empirically that the conclusion still holds near these regions.

We will use this result as follows. In the numerical implementation of (3.3) the initial data and the boundary conditions are determined from (3.1). Then, the computed solution will be compared to a previously computed [1] solution of (3.1).

3.3 Coordinate representation of the second order wave equation

In order to obtain a coordinate representation of (3.3), we introduce a null-tetrad that is adapted to the spherical symmetry of the background metric (2.1). We will choose the same null tetrad $(l^\nu, n^\nu, m^\nu, \bar{m}^\nu)$ as in [1], namely

$$l^\nu = \frac{1}{\sqrt{2}}(1 - t\kappa', \kappa, 0, 0), \qquad n^\nu = \frac{1}{\sqrt{2}}(1 + t\kappa', -\kappa, 0, 0),$$
$$m^\nu = \frac{\mu}{\sqrt{2}}\left(0, 0, 1, -\frac{\mathrm{i}}{\sin\theta}\right), \qquad \bar{m}^\nu = \frac{\mu}{\sqrt{2}}\left(0, 0, 1, \frac{\mathrm{i}}{\sin\theta}\right).$$

The non-vanishing spin-coefficients for this tetrad are

$$\rho = -\rho' = \frac{1}{\sqrt{2}} r\mu', \qquad \varepsilon = \gamma = -\frac{1}{2\sqrt{2}}\kappa'. \tag{3.9}$$

Now we express the wave operator $\Box$ in terms of the weighted differential operators of the GHP (Geroch-Held-Penrose) formalism [17] using the commutation relations

$$\begin{aligned}
&(\text{þ}'\text{þ} - \text{þ}\text{þ}')\phi_{ABCD} = 0, \qquad (\eth\text{þ} - \text{þ}\eth)\phi_{ABCD} = -\rho\,\eth\phi_{ABCD},\\
&(\eth\text{þ}' - \text{þ}'\eth)\phi_{ABCD} = -\rho'\,\eth'\phi_{ABCD}, \qquad (\eth'\eth - \eth\eth')\phi_{ABCD} = 0,
\end{aligned}$$

which contain only the non-vanishing spin-coefficients. Expanding the spin-2 zero-rest-mass field in the familiar way

$$\begin{aligned}
\phi_{ABCD} \equiv\; & \iota_A\iota_B\iota_C\iota_D\phi_0 - 4\,\iota_{(A}\iota_B\iota_C o_{D)}\phi_1 + \\
& + 6\,\iota_{(A}\iota_B o_C o_{D)}\phi_2 - 4\,\iota_{(A} o_B o_C o_{D)}\phi_3 + o_A o_B o_C o_D\phi_4,
\end{aligned}$$

we obtain the following system of five equations

$$\text{þ}\text{þ}'\phi_k - \rho'\,\text{þ}\phi_k - \rho\,\text{þ}'\phi_k + k(5-k)\,\rho^2\,\phi_k = \eth\eth'\phi_k + (4-k)\,\rho\,\eth\phi_{k+1} - k\,\rho\,\eth'\phi_{k-1} \tag{3.10}$$

with $k = 0,1,2,3,4$.

Expressing the GHP operators þ and þ′ in terms of the directional derivatives along the tetrad vectors l and n (see [17]) yields

$$\begin{aligned}
\text{þ}\,\eta &= \frac{1}{\sqrt{2}}\left((1 - t\kappa')\,\partial_t + \kappa\,\partial_r - 2\sqrt{2}\,w\,\varepsilon\right)\eta,\\
\text{þ}'\eta &= \frac{1}{\sqrt{2}}\left((1 + t\kappa')\,\partial_t - \kappa\,\partial_r - 2\sqrt{2}\,w\,\gamma\right)\eta,
\end{aligned}$$

where η is a $\{p,q\}$-scalar quantity with boost-weight $w = \frac{p+q}{2}$ and spin-weight $s = \frac{p-q}{2}$, see [17]. Due to the spherical symmetry of the metric and the adapted null-tetrad it is natural to refer the $\eth$ and $\eth'$ operators to the unit-sphere, so that we replace

$$\eth \mapsto \frac{\mu}{\sqrt{2}}\,\eth, \quad \eth' \mapsto \frac{\mu}{\sqrt{2}}\,\eth'$$

in (3.10) as in [1]. Then the system (3.10) takes the form

$$\begin{aligned}
&(1 - t^2\kappa'^2)\partial_{tt}\phi_k - \kappa^2\partial_{rr}\phi_k + 2t\kappa\kappa'\partial_{tr}\phi_k\\
&\quad + 2\left[(2-k)\kappa' - t(\kappa'^2 + r\mu'\kappa' - \frac{1}{2}\kappa\kappa'')\right]\partial_t\phi_k + 2r\kappa\mu'\partial_r\phi_k\\
&\quad + \left[(2-k)(\kappa\kappa'' + (1-k)\kappa'^2) + k(5-k)r^2\mu'^2\right]\phi_k\\
&\qquad = \mu^2\,\eth\eth'\phi_k + (4-k)\,r\,\mu\,\mu'\,\eth\phi_{k+1} - k\,r\,\mu\,\mu'\,\eth'\phi_{k-1}.
\end{aligned} \tag{3.11}$$

Finally, we use the spherical symmetry of the metric (2.1) to expand the components ϕ_k of the spin-2 field as a sum of spin-weighted spherical harmonics ${}_sY_{lm}$ in the following way

$$\phi_k(t,r,\theta,\phi) = \sum_{lm}\phi_k^{lm}(t,r)\,{}_{2-k}Y_{lm}(\theta,\phi),$$

where $s = 2-k$ is the spin-weight of ϕ_k and the integers s,l,m satisfy the inequalities $|s| \leq l$ and $|m| \leq l$. Since the operators $\eth, \eth'$ act on the spin-weighted spherical harmonics ${}_sY_{lm}$ as

$$\begin{aligned}
\eth({}_sY_{lm}) &= -\sqrt{l(l+1)-s(s+1)}\ {}_{s+1}Y_{lm},\\
\eth'({}_sY_{lm}) &= \sqrt{l(l+1)-s(s-1)}\ {}_{s-1}Y_{lm},\\
\eth\eth'({}_sY_{lm}) &= -(l(l+1)-s(s-1))\ {}_sY_{lm},
\end{aligned}$$

the system (3.11) decouples into separate systems for each mode of the fixed pair (l,m), i.e.

$$\begin{aligned}
&(1-t^2\kappa'^2)\partial_{tt}\phi_k - \kappa^2\partial_{rr}\phi_k + 2t\kappa\kappa'\partial_{tr}\phi_k\\
&\qquad + 2\left[(2-k)\kappa' - t(\kappa'^2 + r\mu'\kappa' - \frac{1}{2}\kappa\kappa'')\right]\partial_t\phi_k + 2r\kappa\mu'\partial_r\phi_k\\
&\qquad + \left[(2-k)(\kappa\kappa'' + (1-k)\kappa'^2) + k(5-k)r^2\mu'^2\right]\phi_k\\
&\qquad\qquad = -\mu^2 c_k^2\phi_k - r\mu\,\mu'((4-k)c_k\,\phi_{k+1} + k\,c_{k-1}\,\phi_{k-1}),
\end{aligned} \tag{3.12}$$

where $c_k = \sqrt{l(l+1)-(2-k)(1-k)}$ whenever the square root is real and otherwise $c_k = 0$. For the sake of simplicity the notation $\phi_k^{lm} = \phi_k$ was introduced. It is worthwhile to mention that this form of the system holds for $l \geq 2$, since for $l = 1$ the components ϕ_0 and ϕ_4 vanish and for $l = 0$ only ϕ_2 survives. Since the above system comes from equations involving the wave operator it is hyperbolic.

3.4 Characteristic curves

Because of its hyperbolic nature the system (3.12) has two families of real characteristic curves. As in the case of the spin-2 equation, their behavior will be very useful in the subsequent numerical studies. Following [8], the slope of the characteristic curves for the system (3.12) is given by

$$\frac{dt}{dr} = \pm\frac{1-t\kappa'(r)}{\kappa(r)}.$$

The characteristic curves of the spin-2 wave equation are identical to those of the spin-2 equation. Fig. 2 shows the 'outgoing' characteristic curves of (3.12) with slope $dt/dr = (1-t\kappa')/\kappa$ near a neighborhood of I^+; near I^- these curves tend to become parallel to the cylinder I. On the other hand, the 'ingoing' characteristic curves with slope $dt/dr = -(1+t\kappa')/\kappa$ are becoming parallel to I near I^+; their behavior in a neighborhood of I^- can be visualized by a reflection of Fig. 2 along the r-axis.

There is a slight difference with the first order case, though. Now, the behavior of the characteristic curves is universal, in the sense that all the components of the spin-2 field propagate along the same characteristics, while in the first order system different components have in general different characteristics (depending on the gauge).

Furthermore, as in the first order system the evolution equation reduce to an interior system on the cylinder in the sense that there remain no r-derivative terms in

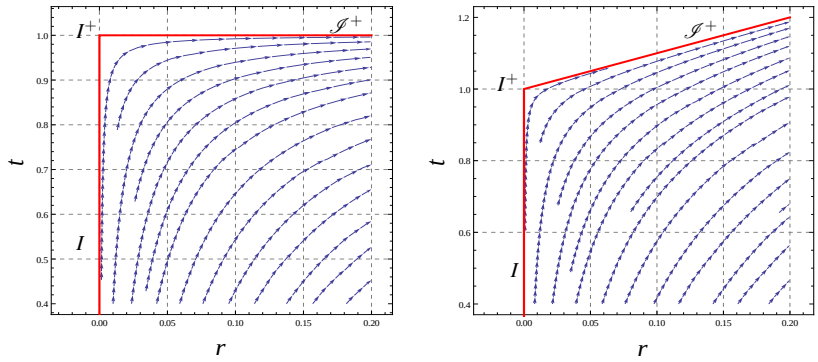

(a) (b)

Fig. 2 Characteristic curves of all the fields ϕ_k in a neighborhood of I^+. The red line denotes the cylinder and null-infinity. The situation close to I^- is obtained by a reflection in the r-axis. (a) Characteristic curves of slope $\frac{dt}{dr} = \frac{1-t}{r}$ in the 'horizontal' case $\mu = 1$. (b) Characteristic curves of slope $\frac{dt}{dr} = \frac{1-t\kappa'}{\kappa}$ in the 'diagonal' case $\mu = \frac{1}{1+r}$.

the equations when evaluated at $r = 0$. So, as before, the cylinder is a total characteristic for the system. And as before, the equations loose their hyperbolicity at $I^{\pm}$, since the coefficient in front of the second time derivative vanishes there.

4 Numerical analysis and results

In this section, we will numerically solve the initial boundary value problem for the spin-2 wave equation (3.12) using the findings of sec. 3.2. Specifically, we will prescribe initial data that satisfy the constraints of the first order system and subsequently evolve them with (3.12). In addition, the boundary conditions will be prescribed using the first order system.

4.1 Numerical implementation

We discretize the $1+1$ system (3.12) (one time and one spatial dimension) using the method of lines. Accordingly, the system (3.12) is reduced to a system of ordinary differential equations by discretizing the spatial coordinate r. In this work, we use finite difference techniques to achieve that.

As computational domain we adopt the interval $D = [0,1]$. A finite representation of D is obtained through the introduction of an equidistant grid $r_i = ih$ with $i = 0,\ldots,N$ on D, where $r_N = 1$, and h is the grid spacing. The spatial derivative operators appearing in (3.12) are approximated by appropriate *summation by parts* (SBP) finite difference operators [3,4,15,19]. The SBP operators arise from discrete versions of the continuous energy estimates that were originally introduced in [10,11]. While these energy estimates guarantee the well-posedness in the continuous case, on the discrete

level their discrete counterparts guarantee the numerical stability of our discrete schemes. This is the main reason we chose to use these specific finite difference operators.

Another very appealing property of the SBP operators is that although their accuracy near the boundaries is, depending on the details of their construction, one or two orders smaller than the one in the interior of the grid, the overall accuracy is of the same order with the accuracy in the interior. Here, we approximate the second derivatives with a minimal width, full norm SBP operator given in [15], which is fourth order accurate in the interior and second order at the boundary. Unfortunately, it was not possible to stabilize the above operator with the corresponding SBP operator of the same norm matrix approximating the first derivatives given in [15]. Instead, we combined it with the SBP operator constructed in [19], which was very successfully used already in the numerical implementation of the first-order formulation of the spin-2 equation, see [1]. Thus, the first derivatives were approximated with a minimum bandwidth, restricted full norm SBP operator of fourth and third order accuracy in the interior and at the boundaries, respectively, taken from [19].

With this choice, we violate the assumption made in [15], of approximating both first and second derivatives with SBP operators of the same norm. Theoretically though, under certain conditions on the norm matrices of the two operators, energy estimates like the one at the end of sec. 4.2 can still be obtained. So it seems that requiring the same norm for first and second order operators is sufficient but not necessary for stability. To thwart any possible objections—emanating from the above complication—concerning the performance of our numerical code we also carried out numerical simulations using (first and second order) SBP operators of the same norm—but one order less accurate than the choice above. Specifically, the second derivatives were approximated by a minimal width, diagonal norm, fourth order accurate in the interior and second order at the boundary SBP operator and the first derivatives by a SBP operator of the same accuracy and norm, both given in [15]. Being constructed for a diagonal norm this combination of operators is expected (see [15]) to have a third order overall accuracy. Our numerical findings, see [5], confirmed this expectation.

A point that also needs special attention is the imposition of the boundary conditions. A wrong imposition of the boundary condition would destroy the designed accuracy of the SBP operators and lead to instabilities [2]. We use a very simple, but highly efficient, *penalty* method—the so-called *simultaneous approximation term* (SAT) method introduced in [2]—that preserves the designed accuracy of the SBP operators and guarantees the numerical stability of our schemes. The combination of the SBP operators with the SAT method has been successfully applied in several different circumstances, see e.g., [2–4, 7, 12, 15, 18].

Finally, one has to decide how to solve the semi-discrete system of ODEs obtained from (3.12) after the spatial discretization. Here, we implement the system as a first-order system of ODEs by introducing the first order time derivatives of the grid functions as additional variables. This system is then solved using the standard 4th order Runge-Kutta scheme.

We choose to work with the first-order system for a number of reasons. Firstly, its numerical implementation is quite simple and very well studied. The imposition of the boundary conditions with the SAT method is also simpler in that case. Furthermore,

a second-order system of ODEs imposes additional restrictions on the construction of SBP operators, which limits the operators available to those with diagonal norm, see [15] for the details.

4.2 Treatment of the boundaries

As it was already mentioned in sec. 3.4, the cylinder is a total characteristic of the system (3.12). Thus, we do not have to prescribe boundary conditions for the points of our computational domain that lie on the cylinder, i.e. at $r = 0$. In contrast, at the boundary $r = 1$ there is one ingoing characteristic for each component of the spin-2 field. Thus, we have to provide appropriate boundary conditions at $r = 1$ for each component ϕ_k. This is an important difference to the first-order spin-2 equation (3.1), where only some of the components propagate inwards and therefore need boundary conditions. We use different boundary conditions which are known to lead to well-posed problems for the wave equation: Neumann or, more generally, Robin conditions of the form

$$\phi_k(t,1) + \partial_r \phi_k(t,1) = g_k(t), \tag{4.1}$$

where $k = 0,\dots,4$, as well as Sommerfeld type boundary conditions. Since we need to use informations from the 1st order formulation of the spin-2 equation (as discussed in sec. 3.2), which provides relations for the values of the first derivatives of the components but not for the values of the functions themselves, we cannot impose Dirichlet conditions.

To motivate the above choice of boundary conditions and to exemplify the use of the SAT method for systems with second derivatives, we will consider the simplest form of a 1-D wave equation

$$u_{tt} = u_{xx}, \qquad 0 \le x \le 1, \quad t \ge 0 \tag{4.2}$$

with homogeneous Robin boundary conditions

$$\alpha\, u(t,0) + u_x(t,0) = 0, \qquad \beta\, u(t,1) + u_x(t,1) = 0,$$

where α, β are arbitrary constants. The energy method for the above boundary value problem gives

$$\frac{d}{dt}\left(\int_0^1 (u_t^2 + u_x^2)\, dx\right) = \frac{d}{dt}\left(-\beta\, u^2(t,1) + \alpha\, u^2(t,0)\right),$$

which leads to an energy estimate when $\beta \ge 0$ and $\alpha \le 0$.

The semi-discrete approximation of eq. (4.2) is $\upsilon_{tt} = D_2 \upsilon$, where $\upsilon = (\upsilon_i)_{i=0:N}$ is the grid function approximating the solution u and the $(N+1)\times(N+1)$ matrix D_2 is the SBP operator approximating the second derivative operator $\partial^2/\partial x^2$. Following [13, 15], the implementation of the boundary conditions with the SAT method leads to the introduction of a couple of boundary terms in the following fashion

$$\upsilon_{tt} = D_2 \upsilon + \tau_0 H^{-1} E_0 (\alpha I + S)\upsilon + \tau_N H^{-1} E_N (\beta I + S)\upsilon,$$

where $E_0 = \mathrm{diag}(1,0,\dots,0)$, $E_N = \mathrm{diag}(0,\dots,0,1)$, $I = \mathrm{diag}(1,\dots,1)$ are matrices of size $(N+1)\times(N+1)$, S is an approximation of the first derivative operator at the boundary, H is the norm matrix of D_2, and τ_0, τ_N are the so-called penalty parameters. The energy method for the above semi-discrete wave equation gives [13, 14]

$$\frac{d}{dt}\left(v_t^T H v_t + v^T A v\right) = \frac{d}{dt}(\tau_0 \alpha v_0^2 + \tau_N \beta v_N^2) + 2(\tau_0 - 1)\dot{v}_0 (Sv)_0 + 2(\tau_N + 1)\dot{v}_N (Sv)_N,$$

where $A = A^T$ is the matrix in the definition of D_2, i.e. $D_2 = H^{-1}(-A + BS)$ with $B = \mathrm{diag}(-1,0,\dots,0,1)$. An energy estimate exists for $\tau_0 = 1, \tau_N = -1$ and (as above) $\beta \geq 0$, $\alpha \leq 0$:

$$\frac{d}{dt}\left(v_t^T H v_t + v^T A v\right) = \frac{d}{dt}(\alpha v_0^2 - \beta v_N^2),$$

which is the semi-discrete analog of the above continuous energy estimate. This procedure for imposing boundary conditions holds true [14] also for Neumann and Sommerfeld conditions, but not for Dirichlet conditions. In that case, as was shown in [14], the method of imposing boundary conditions with the SAT method must be modified in order to guarantee the stability of the numerical scheme. As discussed above, we do not have the need for imposing Dirichlet conditions. Therefore, by choosing (4.1), Neumann or Sommerfeld boundary conditions, we do not have to go into these additional complications.

4.3 The exact solution

As described in sec. 3, the system (3.12) is just a second order reformulation of the spin-2 equation. Therefore, it must be satisfied by the exact solution presented in [1,5]:

$$\begin{aligned}
\phi_0(t,r) &= \frac{r^2(1+r-t)^4}{(1+r)^7}, \qquad \phi_1(t,r) = \frac{2r^2(1+r-t)^3(1+r+t)}{(1+r)^7}, \\
\phi_2(t,r) &= \frac{\sqrt{6}r^2(1+r-t)^2(1+r+t)^2}{(1+r)^7}, \\
\phi_3(t,r) &= \frac{2r^2(1+r-t)(1+r+t)^3}{(1+r)^7}, \qquad \phi_4(t,r) = \frac{r^2(1+r+t)^4}{(1+r)^7}.
\end{aligned} \tag{4.3}$$

Recall that this solution refers to the $l = 2$ mode in the 'diagonal' representation of null-infinity. According to the discussion in sec. 3.2, the initial data must satisfy the constraints of the first order system and be subsequently evolved with the second order system (3.12). Therefore, evaluating (4.3) at $t = 0$, the initial data for each one of the fields are

$$\phi_0(r) = \phi_4(r) = \frac{r^2}{(1+r)^3}, \quad \phi_1(r) = \phi_3(r) = \frac{2r^2}{(1+r)^3}, \quad \phi_2(r) = \frac{\sqrt{6}r^2}{(1+r)^3}. \tag{4.4}$$

In a similar way, i.e. differentiating (4.3) with respect to t and evaluating at $t = 0$, the first temporal derivative of the components of the spin-2 field read

$$\dot{\phi}_0(r) = \dot{\phi}_1(r) = -\dot{\phi}_3(r) = -\dot{\phi}_4(r) = -\frac{4r^2}{(1+r)^4}, \quad \dot{\phi}_2(r) = 0. \tag{4.5}$$

In summary, (4.4) and (4.5) will be our initial conditions in this section. In addition, at $r = 1$, we have to prescribe Robin boundary conditions of the form (4.1). By differentiating (4.3) with respect to the spatial coordinate r and evaluating at $r = 1$ we obtain

$$g_0(t) = -\frac{1}{256}(t-2)^3(6+t), \quad g_1(t) = \frac{1}{128}(48-32t+t^4),$$
$$g_2(t) = -\frac{1}{128}\sqrt{\frac{3}{2}}(t^2-4)(12+t^2),$$
$$g_3(t) = \frac{1}{128}(48+32t+t^4), \quad g_4(t) = -\frac{1}{256}(t-6)(2+t)^3,$$

where the subscript denotes the component of the spin-2 field to which each boundary condition corresponds. The above boundary conditions are imposed with the SAT method.

	ϕ_0		ϕ_4	
Grid	1st order	2nd order	1st order	2nd order
50	-24.8993	-27.1097	-11.3229	-12.2922
100	-29.0579	-31.3535	-13.3223	-15.1472
200	-33.3784	-35.5212	-17.3260	-18.1698
400	-37.7813	-39.6182	-20.4876	-21.2892

Table 1 The logarithm of the normalized l^2 norm of the absolute error E, $\log_2(||E||_2)$, between the exact solution and the solutions computed from the 1st-order system (3.1) and the 2nd-order system (3.3) at time $t = 1$. Note, the 4th order convergence in ϕ_0 and the 3rd-order convergence in ϕ_4.

Evolving the initial data (4.4) and (4.5) with the second order system (3.12) we can reach $t = 1$ without loss of the expected 4th order convergence. In addition, the constraints are preserved during the evolution. The above results strongly indicate that our code reproduces successfully the exact solution (4.3).

But the purpose of this work is to compare the present numerical approach with the one developed in [1], thus a first step towards this goal would be to check which approach reproduces better the exact solution (4.3). Tab. 1 serves this purpose. Specifically, it depicts the logarithm of the normalized l^2 norm of the absolute error E, i.e. $\log_2(||E||_2)$, of the components ϕ_0, ϕ_4 for the two numerical approaches at time $t = 1$. Notice that a slightly better accuracy is achieved in the second order approach.

We have also done the comparisons in the 'horizontal' case with similar results. Here, we cannot reach I^+ due to the degeneracy of the equation at $t = 1$ which affects the numerical algorithm because the propagation speeds grow unboundedly. However, we can come arbitrarily closely to $\mathscr{I}^+$ using an adaptive time-step. We will not go into any further details here because the phenomena are the same as discussed in [1].

4.4 General initial data

According to the results of the preceding section, there is strong evidence that our numerical code converges with the expected order and reproduces successfully the

exact solution (4.3) of the system (3.12). With the confidence that these results provide us, we can proceed further in the numerical study of the spin-2 wave system and seek for numerical solutions, which do not correspond to exact solutions of the system (3.12). In addition, we will confirm numerically the analytic result of sec. 3.2, namely that the solutions of the two different formulations for the spin-2 equation coincide if the initial and boundary data are chosen appropriately.

Again, the initial data satisfy the constraints of the 1st order system and are evolved with the second order system (3.12). We use the constraints in the form derived in sec. 3.3 of [1] to determine the initial values of all the components in terms of one free function. We define the auxiliary variables $\psi_i(r) := \phi_i(r)/\mu(r)^3$ for which the constraints imply the following relationships

$$\begin{aligned} \psi_0(r) = \psi_4(r) &= \frac{-\alpha_0^2\,\psi_2(r) + 2\,r\,\psi_2'(r) + 2\,r^2\,\psi_2''(r)}{\alpha_0\,\alpha_2}, \\ \psi_1(r) = \psi_3(r) &= \frac{r\,\psi_2'(r)}{\alpha_0}, \end{aligned} \tag{4.6}$$

with $\alpha_0 = \sqrt{l(l+1)}$ and $\alpha_2 = \sqrt{l(l+1)-2}$.

This choice leaves the component ϕ_2 completely at our disposal and allows us to compute the remaining components explicitly. Note, that this is not the most general form of the initial data. We have restricted ourselves to the case where $\phi_3(r) = \phi_1(r)$. Otherwise there would exist another free function.

We take the initial values of ϕ_2 in the form of a bump function

$$\phi_2(r) = \begin{cases} \left(4\,\frac{r}{b}(1-\frac{r}{b})\right)^{16}, & 0 \le r \le b \\ 0, & b \le r \le 1 \end{cases}. \tag{4.7}$$

centered at $r = b/2$, then all the other components are bump functions as well. In this section, we will choose $b = 1$.

We also have to specify initially the first time derivatives of the components. The evolution equations of the first order system, see Appendix A, will be used for this purpose. Evaluated at $t = 0$ they read

$$\begin{aligned} \dot\phi_0(r) &= \kappa\,\phi_0'(r) - (3\kappa' - \mu)\,\phi_0(r) - \alpha_2\,\mu\,\phi_1(r), \\ \dot\phi_1(r) &= \frac{1}{2}\,\alpha_2\,\mu\,\phi_0(r) - \frac{1}{2}\,\alpha_0\,\mu\,\phi_2(r) - \mu\,\phi_1, \\ \dot\phi_2(r) &= \frac{1}{2}\,\alpha_0\,\mu\,\phi_1(r) - \frac{1}{2}\,\alpha_0\,\mu\,\phi_3(r), \\ \dot\phi_3(r) &= \frac{1}{2}\,\alpha_0\,\mu\,\phi_2(r) - \frac{1}{2}\,\alpha_2\,\mu\,\phi_4(r) + \mu\,\phi_3(r), \\ \dot\phi_4(r) &= -\kappa\,\phi_4'(r) + (3\kappa' - \mu)\,\phi_4(r) + \alpha_2\,\mu\,\phi_3(r), \end{aligned} \tag{4.8}$$

where the values of the fields on the r.h.s can be evaluated from (4.6), (4.7).

Finally, we explain how we specify the boundary conditions. As discussed in sec. 3.2 we need to use the available information from the first-order system (3.1). In this system there is only one component, namely ϕ_0, which propagates inward from the boundary at $r = 1$. Thus, there is only one free function to be specified on that

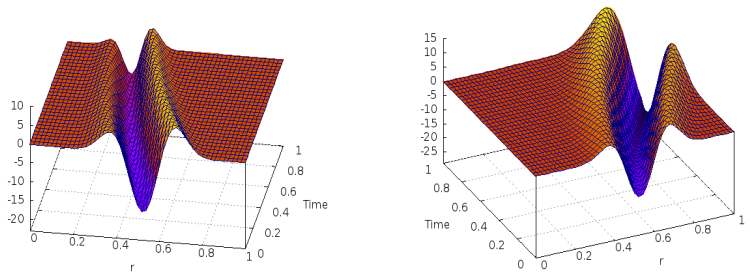

(a) (b)

Fig. 3 The numerical solutions of (a) ϕ_0 and (b) ϕ_4 for the evolution of general initial data—centered around $r = 0.5$—for the $l = 2$ mode in the 'diagonal' representation.

boundary, which characterizes the solution inside given initial data. This must be the case also for the second order system after imposing the boundary conditions.

The second order wave equations require for each component a boundary condition at $r = 1$ (recall that $r = 0$ is a total characteristic so we cannot prescribe any conditions there). We impose these conditions in the form of a Robin condition (4.1)

$$\phi_i(t,1) + \phi_i'(t,1) = g_i(t), \quad i = 0,1,2,3,4.$$

The boundary functions $g_i(t)$ are computed from the first-order system in terms of the fields and their time derivatives. There is no unique way to do this because there are both constraint and evolution equations involving ϕ_1, ϕ_2 and ϕ_3 which could be use for this purpose. We choose to use the constraint equations (A.6-A.8) for ϕ_1, ϕ_2 and ϕ_3 and the evolution equations (A.1) and (A.5) for ϕ_0 and ϕ_4.

Since ϕ_0 is freely specifiable on the boundary we choose it simply as zero, so that ϕ_0 and its time derivative vanish on the boundary. Wherever ϕ_0 appears in the equations used, we simply drop it. The functions $g_i(t)$ are computed by evaluating the left hand side of (4.1) with the spatial derivative substituted from the corresponding first-order equation and putting ϕ_0 and $\dot{\phi}_0$ equal to zero.

The resulting equation for each component is imposed numerically using the SAT method. Note, that we have essentially only rewritten the first-order equation for the components in a superficial form of a Robin condition. We could just as well have chosen a Neumann condition or even a Sommerfeld condition. In all cases the effective boundary condition, i.e., the penalty term to be added to the discretized wave equation would have been the same. In fact, we do not see any difference if we implement the same boundary conditions as Neumann or even as Sommerfeld condition.

We specify initial data for the simplest non-trivial case $l = 2$ in the 'diagonal' representation. For the evolution of the data (4.7), (4.8) described above, the numerical solutions for the 'ingoing' and 'outgoing' components ϕ_0 and ϕ_4, respectively, are presented in Fig. 3. These components satisfy first-order advection equations which are purely ingoing resp. outgoing. These properties are clearly visible in the plots.

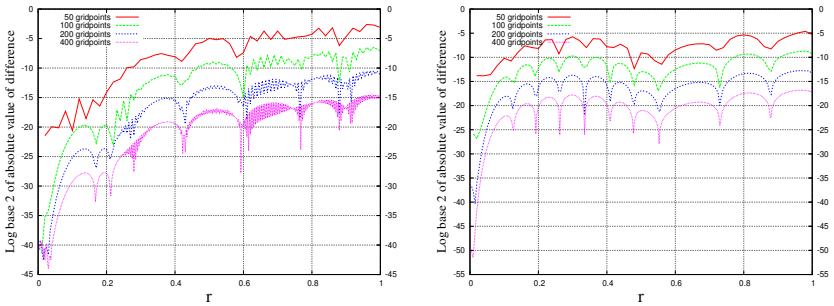

Fig. 4 The convergence plots of ϕ_4 for the evolution of the initial data (4.7), (4.8) in the 'diagonal' representation at time $t = 1$ in (a) the first order approach [1] and (b) the second order approach developed in the present work.

In Fig. 4 we compare the convergence plots of the ϕ_4 component at $t = 1$ obtained from the evolution of the same initial data (4.7) and (4.8) in the two numerical approaches developed in the present work and [1]. More precisely, in Fig. 4(a) the initial data are evolved using the first-order system (A.1)-(A.5), while in Fig. 4(b) the second order system (3.12) is used. In each case, the difference to a high resolution run is computed, which here is 800 grid points. In both cases we find 4th order convergence. Notice, though, that in the second order case the plots look much cleaner. The high frequency features, appearing on the convergence plot of the first order system, are not present in the plot for the second order system. This result confirms the prediction of [9] that the spurious waves will disappear in the second-order formulation.

	ϕ_0		ϕ_4	
Grid	$\log_2(\|\|E\|\|_2)$	Rate	$\log_2(\|\|E\|\|_2)$	Rate
50	-2.5929		-1.2116	
100	-6.4693	3.8764	-5.1393	3.9277
200	-10.3956	3.9263	-9.1361	3.9968
400	-13.8513	3.4557	-13.3382	4.2021

Table 2 Convergence of the solutions to the wave equations towards a solution at high resolution (800 grid points) of the first order equation. The table shows the (logarithms of) the normalized l^2 norm of the absolute differences and the corresponding convergence rates at time $t = 1$.

Now, we reproduce numerically the analytic result of sec. 3.2: we show that if the initial data satisfy the constraints (4.6) of the first order system and are evolved with the second order system (3.12), then the resulting numerical solutions converge (with increasing resolution) to the one obtained by evolving the same initial data with the evolution equations (A.1)-(A.5) of the first order system. To make a connection with the results of Fig. 4, we consider again initial data centered around $r = 0.5$ of the form (4.7), (4.8) and impose boundary conditions as described above. We evolve these data with both evolution systems and compute the absolute error between the numerical solutions of the second order approach and the numerical solution of the

highest resolution (800 grid points) in the first order approach. The normalized l^2 norm of the computed absolute error and the corresponding convergence rates at time $t = 1$ for the components ϕ_0, ϕ_4 are listed in Tab. 2. We find that the solutions agree within numerical accuracy. This confirms the statement made in sec. 3.2 that the two systems have identical solutions given the same initial data.

5 Discussion

In this work we have reformulated the first-order system for the spin-2 field equations for linear gravitational perturbations on Minkowski space as a system of coupled second-order wave equations. The system was implemented into a numerical code and studied under certain simplifying assumptions.

Our first analytical result, see sec. 3.2, is that the first-order system and the second-order system are equivalent if and only if the underlying space-time is conformally flat and has a vanishing scalar curvature. In the case under study the space-time is conformal to Minkowski space-time, i.e., conformally flat and the conformal factor has been chosen in a such a way that the scalar curvature vanishes. Thus, we can evolve the spin-2 field using either the first or the second order system. Given initial and boundary data computed from the first-order system the second-order system provides the same solutions.

Our main goal was the comparison of the numerical properties of the two formulations in the conformal setting given in sec. 2. From the numerical results presented in sections 4.3 and 4.4 we can conclude that we get the same qualitative behaviour of the numerical solutions. In particular, we have shown explicitly that solutions of the second-order system converge to a solution of the first-order system with the same initial and boundary data. The solutions can be evolved stably up to and including I^+ in the diagonal case but not beyond. Any attempt to evolve beyond I^+ with the same algorithm end in numerical instability. In an upcoming paper we will discuss some attempts to circumvent these problems.

Concerning the comparison of the two approaches we confirm the claims in [9]: with the same number of grid points we obtain better accuracy roughly by a factor 4 with the second-order system and we do not see any spurious high-frequency waves in the second-order system.

In our code we have chosen a combination of first and second order discrete operators which are SBP operators with respect to *different* inner products. Our numerical results indicate though that the requirement of using consistent SBP operators that are based on the same norm does not seem to be very restrictive. The fact that we could obtain results of similar accuracy and convergence with the ones presented in secs. 4.3, 4.4 with yet another restricted full norm operator taken from [4] strengthens this statement even more. It seems that the second order full norm operator we are using is performing quite well when combined with first order SBP operators based on a restricted full norm. We have also carried out numerical simulations using (first and second order) SBP operators of the same norm. Our results agree with their designed accuracy as described in [15].

6 Acknowledgments

This work has been supported by Marsden grant UOO0922 of the Royal Society of New Zealand. The authors are grateful to H. Friedrich, O. Reula and M. Tiglio for discussions of separate aspects of this research.

A The first order equations

As a reference, we list here the spin-2 zero-rest-mass equation (3.1) in the formulation used in [1]. The geometry and the notation is exactly the same as described in sec. 3.3. The system consists of eight equations which can be split into the five time evolution equations

$$(1+t\kappa')\partial_t\phi_0 - \kappa\partial_r\phi_0 = -(3\kappa'-\mu)\phi_0 - \mu\alpha_2\phi_1, \tag{A.1}$$

$$\partial_t\phi_1 = -\mu\phi_1 + \frac{1}{2}\mu\alpha_2\phi_0 - \frac{1}{2}\mu\alpha_0\phi_2, \tag{A.2}$$

$$\partial_t\phi_2 = \frac{1}{2}\mu\alpha_0\phi_1 - \frac{1}{2}\mu\alpha_0\phi_3, \tag{A.3}$$

$$\partial_t\phi_3 = \mu\phi_3 + \frac{1}{2}\mu\alpha_0\phi_2 - \frac{1}{2}\mu\alpha_2\phi_4, \tag{A.4}$$

$$(1-t\kappa')\partial_t\phi_4 + \kappa\partial_r\phi_4 = (3\kappa'-\mu)\phi_4 + \mu\alpha_2\phi_3 \tag{A.5}$$

and the three constraint equations

$$-2\kappa\partial_r\phi_1 + 6r\mu'\phi_1 - 2t\kappa'\mu\phi_1 + \alpha_0\mu(1-t\kappa')\phi_2 + \alpha_2\mu(1+t\kappa')\phi_0 = 0, \tag{A.6}$$

$$-2\kappa\partial_r\phi_2 + 6r\mu'\phi_2 + \alpha_0\mu(1-t\kappa')\phi_3 + \alpha_0\mu(1+t\kappa')\phi_1 = 0, \tag{A.7}$$

$$-2\kappa\partial_r\phi_3 + 6r\mu'\phi_3 + 2t\kappa'\mu\phi_3 + \alpha_0\mu(1+t\kappa')\phi_2 + \alpha_2\mu(1-t\kappa')\phi_4 = 0. \tag{A.8}$$

References

1. Beyer, F., Doulis, G., Frauendiener, J., Whale, B.: Numerical space-times near space-like and null infinity. The spin-2 system on Minkowski space. Classical and Quantum Gravity **29**(24), 245,013 (2012)
2. Carpenter, M.H., Gottlieb, D., Abarbanel, S.: Time-stable boundary conditions for finite-difference schemes solving hyperbolic systems: methodology and application to high-order compact schemes. J. Comp. Phys. **111**(2), 220–236 (1994)
3. Carpenter, M.H., Nordström, J., Gottlieb, D.: A Stable and Conservative Interface Treatment of Arbitrary Spatial Accuracy. J. Comp. Phys. **148**(2), 341–365 (1999)
4. Diener, P., Dorband, E., Schnetter, E., Tiglio, M.: Optimized High-Order Derivative and Dissipation Operators Satisfying Summation by Parts, and Applications in Three-dimensional Multi-block Evolutions. J Sci Comput **32**(1), 109–145 (2007)
5. Doulis, G.: The generalised conformal field equations near spatial infinity. Ph.D. thesis, University of Otago (2012)
6. Friedrich, H.: Gravitational fields near space-like and null infinity. J. Geom. Phys. **24**, 83–163 (1998)
7. Gong, J., Nordström, J.: Interface procedures for finite difference approximations of the advection-diffusion equation. J. Comp. Appl. Math. **236**(5), 602–620 (2011)
8. John, F.: Partial Differential Equations. Springer-Verlag, Heidelberg (1982)
9. Kreiss, H.O., Ortiz, O.E.: Some mathematical and numerical questions connected with first and second order time-dependent systems of partial differential equations. In: J. Frauendiener, H. Friedrich (eds.) The conformal structure of space-times: geometry, analysis, numerics, pp. 359–370. Springer-Verlag, Heidelberg (2002)
10. Kreiss, H.O., Scherer, G.: Finite element and finite difference methods for hyperbolic partial differential equations. In: Mathematical Aspects of Finite Elements in Partial Differential Equations, pp. 195–212. Academic Press (1974)

11. Kreiss, H.O., Scherer, G.: On the existence of energy estimates for difference approximations for hyperbolic systems. Tech. rep., Dept. of Scientific Computing, Uppsala University (1977)
12. Lehner, L., Reula, O., Tiglio, M.: Multi-block simulations in general relativity: high-order discretizations, numerical stability and applications. Classical and Quantum Gravity **22**(24), 5283 (2005)
13. Mattsson, K.: Summation by Parts Operators for Finite Difference Approximations of Second-Derivatives with Variable Coefficients. J Sci Comput **51**, 650–682 (2012)
14. Mattsson, K., Ham, F., Iaccarino, G.: Stable Boundary Treatment for the Wave Equation on Second-Order Form. J Sci Comput **41**, 366–383 (2009)
15. Mattsson, K., Nordström, J.: Summation by parts operators for finite difference approximations of second derivatives. J. Comp. Phys. **199**(2), 503–540 (2004)
16. Penrose, R.: Zero rest-mass fields including gravitation: asymptotic behaviour. Proc. Roy. Soc. London A **284**, 159–203 (1965)
17. Penrose, R., Rindler, W.: Spinors and Spacetime, vol. 1. Cambridge University Press, Cambridge (1984)
18. Schnetter, E., Diener, P., Dorband, E.N., Tiglio, M.: A multi-block infrastructure for three-dimensional time-dependent numerical relativity. Classical and Quantum Gravity **23**(16), S553–S578 (2006)
19. Strand, B.: Summation by parts for finite difference approximations for d/dx. J. Comp. Phys. **110**(1), 47–67 (1994)
20. Valiente Kroon, J.A.: Polyhomogeneous expansions close to null and spatial infinity. In: J. Frauendiener, H. Friedrich (eds.) The conformal structure of space-time, pp. 135–159. Springer, Berlin (2002)